

## Transient Molecular-Ion Formation in Rydberg-Electron Capture

K. B. MacAdam, J. C. Day, J. C. Aguilar, D. M. Homan, A. D. MacKellar, and N. J. Cavagnero

University of Kentucky, Lexington, Kentucky 40506-0055

(Received 17 April 1995)

Resonance structure has been observed in total cross sections for the capture of an electron from a Rydberg-state atom by a singly charged projectile with speed  $v_{\text{ion}}$  comparable to the Bohr velocity  $v_e$  of the target electron. Prominent peaks in the data at reduced velocities  $\tilde{v} = v_{\text{ion}}/v_e = 0.8$  and  $0.5$  result from two distinct capture mechanisms in which the target electron passes once or three times, respectively, through the midplane between the nuclei. The three-swap peak at  $\tilde{v} = 0.5$  marks the high-velocity limit of molecular-ion formation in which the electron is shared between the two charge centers. This result illustrates that new paradigms for collision dynamics may emerge when reactions are examined at or near the correspondence principle limit.

PACS numbers: 34.60.+z, 34.10.+x, 34.70.+e

Electron capture by a singly charged structureless projectile from a hydrogenlike target remains a fundamental problem of atomic-collision physics. The total cross section  $\sigma$  for the prototype case of capture by protons from ground-state hydrogen atoms is smooth and featureless in the intermediate-energy range near 25 keV/u, where the reduced velocity  $\tilde{v} = v_{\text{ion}}/v_e \approx 1$  [1]. ( $v_e$  is the Bohr orbital velocity of the electron in its initial state.) For target atoms with arbitrary principal quantum numbers  $n$ , where  $v_e = n^{-1}$  a.u., this velocity region is a watershed between perturbative physics at  $\tilde{v} > 1$  and the physics of formation of a transient molecular-ion complex at  $\tilde{v} < 1$  [1,2].

We have discovered peaks and dips in total cross sections for single-electron capture by  $\text{Na}^+$ ,  $\text{K}^+$ , and  $\text{Cs}^+$  ions incident on  $\text{Na}(24d)$  and  $\text{Na}(25s)$  Rydberg states in the reduced velocity range  $0.25 \leq \tilde{v} \leq 1.2$  [3]. When plotted versus reduced velocity (as opposed to energy) the cross sections are independent of the projectile ion. (All singly charged projectiles moving with the same speed exert the same time-dependent force on the target electron.) For all projectiles studied, the cross section  $\sigma(\tilde{v})$  has a narrow peak near  $\tilde{v} = 0.5$  and a broader peak near  $\tilde{v} = 0.8$ . Furthermore, for  $\text{Na}^+$  projectiles, the peaks have been observed for a wide range of initial  $nd$  and  $ns$  states with  $20 \leq n \leq 40$  [4]. The  $n$  independence of the observed structure indicates that the phenomena depend only on the ratio of the speeds of projectile and electronic motion. In classical systems this behavior results from a property of mechanical similarity [5]. In this Letter, we demonstrate that the  $\tilde{v} = 0.5$  peak results from collision processes in which the electron is passed to the projectile, then back to the target, and finally and irreversibly back to the projectile—in a low-velocity analog (referred to here as three-swap capture) of the Thomas mechanism [6]. This peak marks the onset, for decreasing ion speeds, of formation of transient molecular-ion states, in which the electron passes many times between the charge centers.

The experiment is illustrated schematically in Fig. 1. Two-step pulsed-laser excitation at 20-Hz repetition rate was used to produce about  $10^3$  Na Rydberg atoms in a thermal atomic beam, leading first to the  $3^2P_{1/2}$  intermediate state at 589.6 nm and then to  $n^2D_{3/2}$  or  $n^2S_{1/2}$  at about 410 nm. The peak at  $\tilde{v} = 0.5$  responds to variations in the alignment of the  $24d$  target state (Ref. [7], Fig. 3) which can be controlled by varying the plane of polarization of the blue laser beam that is used to excite the target from the  $\text{Na}(3p)$  intermediate state [8]. Both lasers were linearly polarized parallel to the incident ion beam. In the case of  $nd$  initial states the lasers excited a mixed state comprising 60%  $m_\ell = 0$  and 40%  $|m_\ell| = 1$  with reference to this axis [8]. For  $nd$  states parallel polarization resulted in the most pronounced structure in  $\sigma(\tilde{v})$ . The  $ns$  wave function is isotropic and independent of laser polarization.

The Rydberg-state target was exposed to a 1–3 nA ion beam for about  $1 \mu\text{s}$  after each laser pulse. Ions were produced by thermionic-emitter ion sources [9] and were accelerated to 50–2000 eV. The peak at  $\tilde{v} = 0.5$  in the  $\text{Na}(24d)$  target occurs at 250, 420, and 1430 eV for  $\text{Na}^+$ ,

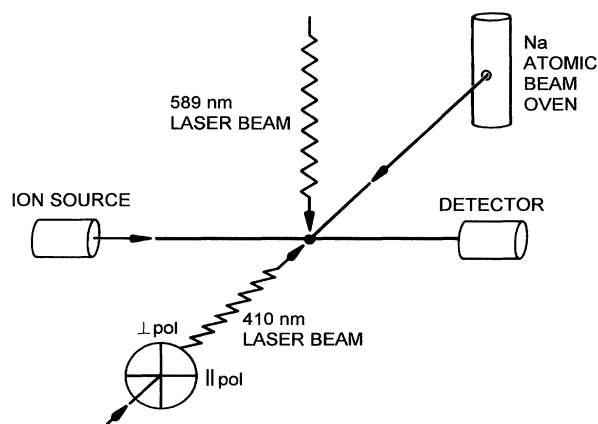


FIG. 1. Experimental apparatus (schematic).

$K^+$ , and  $Cs^+$  ions, respectively. In order to reduce error from energy-dependent variations in beam overlap, the ion beam was pseudorandomly deflected across the target during the measurements [10]. A detector beyond the target region registered the arrival of fast neutrals formed by electron capture in the Rydberg target but blocked those formed by capture in the  $10^{-7}$  Torr rest gas of the chamber [4]. Events from small amounts of unwanted ion species were eliminated by time-of-flight methods.

For normalization of the capture counts, the target atoms were measured by selective field ionization (SFI) [4]. The relative cross section was obtained from  $\sigma = N/iR$ , where  $N$  is the background-corrected number of capture events,  $i$  is the ion beam current, and  $R$  is the integrated SFI signal from the Rydberg atoms in the target.

Several precautions were necessary to ensure a relatively pure target state. Helmholtz coils were used to reduce stray magnetic fields and prevent scrambling of the  $m_\ell$  components of the target. Low target densities were maintained to minimize state mixing due to collisions between target atoms. The apparatus was cooled to liquid-nitrogen temperatures to minimize blackbody depopulation of the initial state. The lower limit of projectile velocity was imposed by the 50-V minimum of acceleration voltage necessary to bring a sufficient ion-beam intensity to the target. Tests with the  $Cs^+$  beam suggested that future studies of cross-section structure may be possible at  $\tilde{v} \geq 0.1$  for  $n \approx 24$  provided that contamination from other alkali ions in the beam is prevented.

The experimental capture velocity dependences  $\sigma(\tilde{v})$  for  $K^+$  on Na(24d) and Na(25s) targets are shown in Fig. 2. Because of the  $s$ - and  $d$ -state quantum defects in Na,  $\delta_s = 1.35$  and  $\delta_d = 0.01$ , these two target states have nearly identical effective quantum numbers  $n^* = n - \delta_\ell = 23.65$  and 23.99, respectively. The scatter of points is a measure of statistical error and run-to-run variations. After a sharp decrease in  $\sigma$  between  $\tilde{v} = 0.25$  and 0.35, small peaks occur at  $\tilde{v} = 0.5$  and 0.8. Both  $s$  and  $d$  states exhibit these peaks, but those for  $d$ -state targets are much sharper and more intense. Structure in the  $s$ -state cross sections resembles that for a nonaligned  $d$  state, which can be produced by setting the 410-nm polarization at the "magic angle,"  $54.7^\circ$  from the ion beam [8]. The capture cross section for the 25s state exceeds that for 24d between  $\tilde{v} = 0.3$  and 0.8 by about 30%. The peaks at  $\tilde{v} = 0.5$  and 0.8 (for a wide range of principal quantum numbers [4]) have survived every attempt to attribute them to spurious causes and are a robust feature of the data. There is no comparable structure visible in  $p + H(1s)$  capture in the corresponding energy range 4–25 keV [1].

The structure in the cross sections indicates the existence of alternative channels contributing to charge transfer in this velocity region. The fact that the observed structure is independent of  $n$  suggests, via the correspondence principle [11,12], that these charge transfer chan-

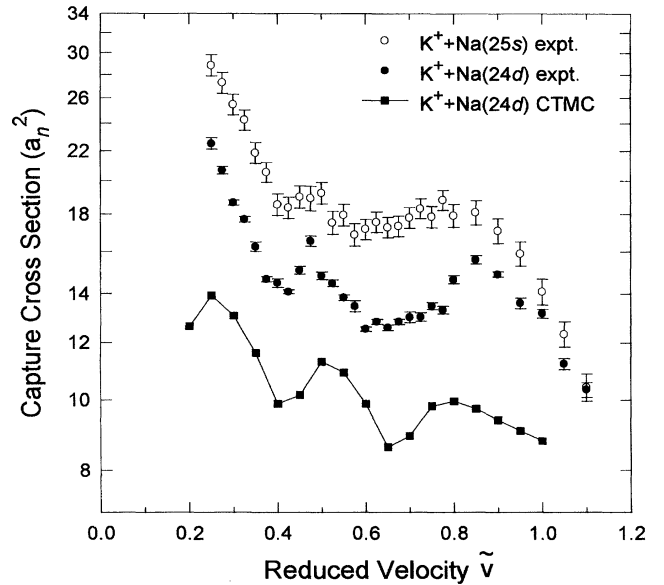


FIG. 2. Total electron-capture cross sections. The CTMC calculations are absolute, corresponding to the scale at the left. (Units  $a_n^2 = n^4 a_0^2$ , where  $a_0$  is the Bohr radius.) The 24d and 25s experimental data are shown with their relative magnitudes as measured and are placed at an arbitrary factor above the theory for clarity.

nels should have classical analogs that can be traced to topologically distinct classes of trajectories. A measure introduced by Homan, Cavagnero, and Harmin [13] that distinguishes alternative collision channels leading to electron capture is used here to reveal that the cross-section structure derives from a peak in the number of three-swap trajectories at  $\tilde{v} = 0.5$  and of one-swap trajectories near  $\tilde{v} = 0.8$ . The three-swap electron trajectories cross the moving midplane between the equally charged force centers *exactly 3 times* during approach and passage of the projectile. (In the limit of high  $\tilde{v}$  this three-swap channel becomes identical to capture by double scattering [6] or "Thomas capture.") The one-swap trajectories, which may be termed "direct capture," correspond to a single passage of the electron across the midplane from the target to the projectile side and can be calculated at high  $\tilde{v}$  in the first Born approximation [1,2].

Our calculations were performed using a standard classical trajectory Monte Carlo (CTMC) algorithm [14] for sampling initial conditions of the target electron (and of the projectile ion) in order to mimic the momentum distribution of the initial Rydberg state. (60 000 trajectories were calculated for each  $\tilde{v}$ , which resulted in statistical errors less than 1% for total charge transfer cross sections and less than 2% for three-swap cross sections.) To account for the dependence of the cross sections on laser

polarization, the CTMC algorithm was modified [15] to restrict the orientation of the initial orbital plane by defining the angle  $\theta$  between the angular momentum vector and the beam axis as

$$\cos\theta = \frac{|m| + \eta - \frac{1}{2}}{\ell + \frac{1}{2}} C, \quad (1)$$

where  $\eta$  is a random number between zero and one. The coefficient  $C = 1$  if  $m \geq 0$ , and  $C = -1$  if  $m < 0$ . The algorithm was further modified to count the number of times (or swaps) that the electron passed through the midplane between the nuclei for each trajectory.

The results of our trajectory calculations are compared with the experimental data in Fig. 2. For this comparison cross sections were calculated separately for each  $m_\ell$ , and the resulting sublevel cross sections were combined in the proportions that represented the mixed target state. (Note that the experimental cross sections are relative; they have not been normalized to the theoretical curve but have been displaced above the latter on the logarithmic scale for clarity. The  $24d$  and  $25s$  data are presented in their experimentally determined ratio.) The CTMC calculation has three peaks at reduced velocities of  $\tilde{v} = 0.25, 0.5$ , and  $0.8$ , and the shape of the classical cross section qualitatively reproduces the experimentally observed structure. The origin of the peaks in the classical calculation is illustrated in Fig. 3, where contributions to charge transfer from one-swap, three-swap, and five- (or more) swap trajectories are plotted versus reduced velocity. The peaks at  $\tilde{v} = 0.5$  and  $0.8$  are clearly

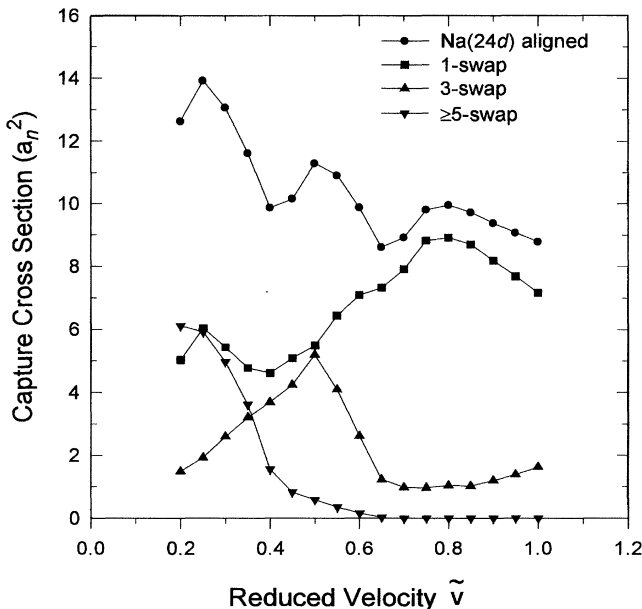


FIG. 3. Multiple-swap contributions to the CTMC capture cross section corresponding to the aligned Na( $24d$ ) target prepared by blue laser whose plane of polarization is parallel to the ion beam (see text and Fig. 1).

identified with enhancements of three-swap and one-swap captures, respectively, in this velocity region.

Our conclusions regarding classical charge transfer channels are remarkably insensitive to the details of the algorithm that samples initial conditions. We have studied the same collision process using an elementary method [16] in which the target atom is modeled as single ellipse with fixed eccentricity  $e = 0.9946$  (corresponding to an angular momentum quantum number  $\ell = 2$  in  $n = 24$ ) and with an orbital plane determined by  $\cos\theta = m/(\ell + \frac{1}{2})$ . This elementary model yields a  $\tilde{v}$  dependence (not shown) of the charge transfer cross section and a separation according to the number of swaps that is nearly identical to those obtained with the full CTMC algorithm.

In earlier theoretical work on charge transfer from circular Rydberg atoms, it was argued [16] that contributions to capture at intermediate velocities could be separated into one-swap and three-swap channels and that the three-swap channel was identical to the Thomas mechanism in the limit of high velocities. In experimentally measuring and theoretically identifying the peak in  $\sigma$  at  $\tilde{v} = 0.5$  we have now demonstrated that the double-scattering mechanism that dominates charge transfer cross sections at high velocity evolves into three-swap capture at much lower velocities where it yields a distinct peak in  $\sigma(\tilde{v})$ .

Quantum mechanical calculations of the capture processes reported here are not yet possible. The complexities associated with the large numbers of target and projectile states excited in collisions with a Rydberg atom are compounded by the strong coupling of molecular states characteristic of the intermediate velocity regime. In low-velocity charge transfer from ground state atoms, the electron density oscillates many times between the charge centers at rates that depend on energy splittings between the molecular-ion states. A similar description of processes involving *only a few swaps* of the electron between charge centers would likely require an extremely large number of molecular states. The manner in which known mechanisms [17] for nonadiabatic transitions between molecular states conspire to produce the essentially classical phenomenon described in this Letter is not yet understood.

The  $\tilde{v} = 0.5$  peak in this work provides an experimental signature not visible in  $p + H(1s)$  capture by which the utility of a description in terms of a small number of adiabatic states can be gauged. In this sense, our observation of the three-swap capture events places an upper limit on the reduced velocity at which the capture process can be regarded as resulting from the transient formation of molecular ion states.

In conclusion, charge transfer experiments at high principal quantum number have been used simultaneously (1) to identify three-swap (Thomas-like) capture at low velocity and (2) to determine experimentally the high-velocity limit of the applicability of the molecular approach to

electron capture. In this way, the study of electron capture from Rydberg atoms may provide critical insight in the velocity regime in which neither low nor high velocity models of charge transfer are valid.

The experimental phase of this work was supported in part by NSF Grant No. PHY-9122377, and the theoretical portions were supported in part by the Division of Chemical Sciences, Office of Basic Energy Sciences, Office of Energy Research, U.S. Department of Energy. J.C.D. was supported by a GAANN Fellowship from the U.S. Department of Education under Grants No. P200A10202 and No. P200A40523. We also gratefully acknowledge computational assistance by the University of Kentucky Center for Computational Sciences.

- 
- [1] B. H. Bransden and M. R. C. McDowell, *Charge Exchange and the Theory of Ion-Atom Collisions* (Clarendon Press, Oxford, 1992).
- [2] B. H. Bransden, *Atomic Collision Theory* (Benjamin/Cummings, Reading, MA, 1983).
- [3] Preliminary reports of experimental work have appeared in Refs. [4,7].
- [4] S. B. Hansen, L. G. Gray, E. Horsdal-Pedersen, and K. B. MacAdam, *J. Phys. B* **24**, L315 (1991). When initially observed for  $20 \leq n \leq 40$  the peaks were indistinct and their origin was unknown.
- [5] L. D. Landau and E. M. Lifshitz, *Mechanics* (Pergamon Press, Oxford, 1976), 3rd ed., p. 22.
- [6] R. Shakeshaft and L. Spruch, *Rev. Mod. Phys.* **51**, 369 (1979).
- [7] K. B. MacAdam, in *The Physics of Electronic and Atomic Collisions*, edited by Torkild Andersen, Bent Fastrup, Finn Folkmann, Helge Knudsen, and N. Andersen, AIP Conf. Proc. No. 295 (AIP, New York, 1993), p. 183.
- [8] K. B. MacAdam and M. A. Morrison, *Phys. Rev. A* **48**, 1345 (1993).
- [9] Spectra-Mat Inc., 1240 Highway 1, Watsonville, CA 95076.
- [10] K. B. MacAdam, N. L. S. Martin, D. B. Smith, R. G. Rolfes, and D. Richards, *Phys. Rev. A* **34**, 4661 (1986).
- [11] I. C. Percival and D. Richards, *Adv. At. Mol. Phys.* **11**, 1 (1975).
- [12] E. Merzbacher, *Quantum Mechanics* (J. Wiley, New York, 1961).
- [13] D. M. Homan, M. J. Cavagnero, and D. A. Harmin, *Phys. Rev. A* **50**, R1965 (1994).
- [14] R. L. Becker and A. D. MacKellar, *J. Phys. B* **17**, 3923 (1984).
- [15] A. D. MacKellar and R. L. Becker, in *Abstracts on Contributed Papers, XIII International Conference on the Physics of Electronic and Atomic Collisions*, edited by J. Eichler *et al.* (Elsevier, New York, 1983), p. 660.
- [16] D. M. Homan, M. J. Cavagnero, and D. A. Harmin, *Phys. Rev. A* **51**, 2075 (1995).
- [17] S. Yu. Ovchinnikov and E. A. Solov'ev, *Zh. Eksp. Teor. Fiz.* **90**, 921 (1986) [*Sov. Phys. JETP* **63**, 538 (1986)].